DENTAL MATERIALS 35 (2019) 523–533

Available online at www.sciencedirect.com

ScienceDirect

journal homepage: www.intl.elsevierhealth.com/journals/dema

# Design and characterization of a chitosan-enriched fibrin hydrogel for human dental pulp regeneration

*Maxime Ducret*[a,b,c], *Alexandra Montembault*[d], *Jérôme Josse*[e], *Marielle Pasdeloup*[a], *Alexis Celle*[a], *Rafiqa Benchrih*[d], *Frédéric Mallein-Gerin*[a], *Brigitte Alliot-Licht*[f,g,h], *Laurent David*[d], *Jean-Christophe Farges*[a,b,c,*]

[a] *Laboratoire de Biologie Tissulaire et Ingénierie thérapeutique, UMR5305 CNRS/Université Lyon 1, UMS3444 BioSciences Gerland-Lyon Sud, Lyon, France*
[b] *Université de Lyon, Université Lyon 1, Faculté d'Odontologie, Lyon, France*
[c] *Hospices Civils de Lyon, Service d'Odontologie, Lyon, France*
[d] *Université de Lyon, Université Lyon 1, CNRS, Ingénierie des Matériaux Polymères (IMP), UMR5223, Villeurbanne, France*
[e] *CIRI — Centre International de Recherche en Infectiologie, INSERM U1111/CNRS UMR5308/ENS Lyon/Université Lyon 1, Lyon, France*
[f] *Centre de Recherche en Transplantation et Immunologie, INSERM UMR1064, Université de Nantes, Nantes, France*
[g] *Université de Nantes, Faculté d'Odontologie, Nantes, France*
[h] *CHU de Nantes, Service d'Odontologie Conservatrice et Pédiatrique, Nantes, France*

ARTICLE INFO

*Article history:*
Received 28 August 2018
Received in revised form
19 December 2018
Accepted 3 January 2019

*Keywords:*
Regenerative dentistry
Tissue engineering
Hydrogel
Fibrin
Chitosan
Antibacterial effect
Dental pulp mesenchymal stem/stromal cells
Cell viability
Proliferation
Collagen synthesis

ABSTRACT

*Objective.* Regenerating a functional dental pulp in the pulpectomized root canal has been recently proposed as a novel therapeutic strategy in dentistry. To reach this goal, designing an appropriate scaffold able to prevent the growth of residual endodontic bacteria, while supporting dental pulp tissue neoformation, is needed. Our aim was to create an innovative cellularized fibrin hydrogel supplemented with chitosan to confer this hydrogel antibacterial property.

*Methods.* Several fibrin–chitosan formulations were first screened by rheological analyses, and the most appropriate for clinical use was then studied in terms of microstructure (by scanning electron microscopy), antimicrobial effect (analysis of *Enterococcus faecalis* growth), dental pulp-mesenchymal stem/stromal cell (DP-MSC) viability and spreading after 7 days of culture (LiveDead® test), DP-MSC ultrastructure and extracellular matrix deposition (transmission electron microscopy), and DP-MSC proliferation and collagen production (RT-qPCR and immunohistochemistry).

*Results.* A formulation associating 10 mg/mL fibrinogen and 0.5% (w/w), 40% degree of acetylation, medium molar mass chitosan was found to be relevant in order to forming a fibrin–chitosan hydrogel at cytocompatible pH (# 7.2). Comparative analysis of fibrin-alone and fibrin–chitosan hydrogels revealed a potent antibacterial effect of the chitosan in the fibrin network, and similar DP-MSC viability, fibroblast-like morphology, proliferation rate and type I/III collagen production capacity.

* *Corresponding author at*: Laboratoire de Biologie Tissulaire et Ingénierie thérapeutique, UMR5305 CNRS/UCBL, Institut de Biologie et Chimie des Protéines, 7 passage du Vercors, 69367 Lyon Cedex 07, France.
E-mail address: jean-christophe.farges@univ-lyon1.fr (J.-C. Farges).
https://doi.org/10.1016/j.dental.2019.01.018

*Significance.* These results indicate that incorporating chitosan within a fibrin hydrogel would be beneficial to promote human DP tissue neoformation thanks to chitosan antibacterial effect and the absence of significant detrimental effect of chitosan on dental pulp cell morphology, viability, proliferation and collagenous matrix production.



## 1. Introduction

Previous studies have shown that the survival rate is lower for endodontically-treated teeth compared to their living counterparts. This has been attributed to the absence of the dental pulp (DP) immune defence, sensory system, and repair/regenerative capacity which makes the tooth more susceptible to re-infection and/or fracture [1,2]. In this context, therapeutic strategies aiming at regenerating a functional DP in the devitalized endodontic space recently received great attention [3–7]. Among the various approaches tested, the cell-based regenerative one has given promising results [8]. This approach relies on the injection, into the endodontic space, of a cellular product made of stem/precursor cells embedded in a tridimensional scaffold, functionalized or not with bioactive molecules. Important clinical and biological requirements for a cellularized scaffold to be used in DP regeneration include easy handling allowing for a rapid implantation into the endodontic space by the dental practitioner (within minutes), low viscosity for a good injectability into such a small-sized space, antibacterial properties to prevent the growth of residual endodontic bacteria, physiological degradation by host and/or encapsulated cells, and rapid replacement with an extracellular matrix (ECM) characteristic of the DP tissue. Numerous kinds of scaffolds have been tested including natural and synthetic polymers/co-polymers, hydroxyapatite/tricalcium phosphate powders, self-assembling peptide systems, and platelet-rich plasma [9–14]. So far, none of these scaffolds was found to possess the structural and functional properties of an ideal biomaterial for DP regeneration, and designing innovative formulations is clearly required [7,10,15].

Fibrin is a natural, insoluble protein which is produced following fibrinogen polymerization under thrombin control during blood clot formation. It forms a fibrous network important for hemostasis and subsequent wound healing [16]. Used as a scaffold, fibrin was recently found to be highly suitable for DP regeneration since it clearly supports pulp-like tissue formation [17]. Its advantages include excellent cytocompatibility and physiological degradation kinetics, non-toxicity of degradation products, and replacement with cell-derived ECM within a few days [18]. Mechanical properties of fibrin scaffolds can be easily fine-tuned by controlling fibrinogen concentration and ionic strength, in order to obtain (i) viscoelastic properties similar to that of connective tissue ECM, (ii) fast diffusion of nutrients and metabolites, and (iii) homogeneous cell encapsulation [18]. However, the absence of antibacterial activity of fibrin or of its by-products during the degradation process [19] may constitute an important limitation, because microorganisms remaining in the endodontic space and dentin tubules may hinder the DP regeneration process [20–22]. This limitation could be overcome by incorporating antibacterial agents to the fibrin scaffold. Among these, chitosan has received considerable attention for over 30 years [23,24]. Chitosan is a natural polysaccharide biopolymer obtained by N-deacetylation of chitin, a major structural component of the exoskeleton of arthropods and insects, the endoskeleton of cephalopods, and fungal cell walls [25]. It is known to possess antimicrobial activity against a variety of gram-negative and gram-positive bacteria, including *Enterococcus fæcalis*, a pathogen frequently found in persistent root canal infections [25–28]. Mechanisms responsible for this activity are not fully understood but may include: the interference of the positively charged chitosan molecules with the negatively charged residues on the bacterial surface, the interaction of diffused hydrolysis products with microbial DNA (which leads to the inhibition of the mRNA and protein synthesis), the chelation of nutrients and essential metals, and the formation of a polymer membrane on the cell surface which prevents nutrients or oxygen from entering the cell [29]. Chitosan could thus be a good candidate as an antibacterial agent, provided that it keeps its antimicrobial properties upon incorporation into the fibrin scaffold.

The aim of this study was to design an injectable hydrogel-type scaffold associating fibrin and chitosan in a formulation which preserves chitosan antibacterial properties, while not affecting dental pulp-mesenchymal stem/stromal cell (DP-MSC) viability, spreading and proliferation, and DP-like ECM deposition within the hydrogel.

## 2. Materials and methods

### 2.1. Reagents

Human fibrinogen (ref. F3879) and thrombin (ref. T6884) were purchased from Sigma-Aldrich (Saint-Louis, USA), and highly deacetylated shrimp shell chitosan (batch type 243) from Mahtani Chitosan® (Gujarat, India). The chemically defined cell culture medium SPE-IV/EBM® and human placental collagens I and III were obtained from ABCellBio (Paris, France), the anti-MKI67 rabbit recombinant monoclonal antibody (clone SP6, ref. M3062) from Eurobio (Courtabœuf, France), the anti-type I collagen rabbit polyclonal antibody (ref. 20111[380k]) and the anti-type III collagen mouse monoclonal antibody (clone 8D1-8C7, ref. 60315[316f]) from Novotec (Bron, France).

### 2.2. Preparation and characterization of the chitosan solution, fibrin hydrogels and fibrin–chitosan hydrogels

The commercial chitosan was dissolved and filtered successively through 3, 0.8 and 0.45 μm Millipore® membranes to

obtain a high-purity material [30] which was characterized by $^{1}H$ nuclear magnetic resonance (NMR) spectroscopy and size exclusion chromatography coupled online with a differential refractometer (Wyatt Optilab T-rEx) and a multi angle laser light scattering detector (Wyatt HELEOS) [31]. Results indicated that this chitosan had an initial degree of acetylation (DA) of 1.5 ± 0.2% and a weight-average molar mass (Mw) of 160 ± 10 kg/mol with a dispersity index Đ of 1.9 ± 0.2 (Đ = Mw/Mn). This polymer was then *N*-reacetylated to reach a DA of 40% using acetic anhydride as a reactive, as previously described [32]. Briefly, chitosan was dissolved at a concentration of 0.5% (w/v) in a water/1,2-propanediol mixture (1/1 [v/v]). Acetic anhydride was then diluted in 1,2-propanediol and this resulting acetylating reactive was added dropwise to the chitosan solution. The amount of acetic anhydride added corresponded to the stoichiometric amount necessary to achieve the required degree of acetylation. The medium was let to stand for 3 h. The *N*-reacetylated chitosan was then isolated by precipitation with aqueous ammonia, thoroughly washed with deionized water until neutral pH, and freeze-dried.

For the fibrin–chitosan hydrogel preparation, a 1% [w/w] DA40% chitosan solution was prepared by dissolving overnight the lyophilized polymer powder in a deionized aqueous solution of acetic acid. The quantity of acid added corresponded to the amount necessary to reach the protonation of the free amine site of D-glucosamine residues in the aqueous acidic solution. The pH of the chitosan solution was then increased to a cytocompatible level (7.1–7.2) by adding sodium hydroxide while avoiding chitosan precipitation. The final chitosan solution was sterilized by autoclaving at 121 °C for 20 min. The viscosity of 0.2–1% chitosan solutions was then assessed in a static mode with an AR2000 rheometer (TA instruments, New Castle, DE, USA), by using a coaxial cylinder-cylinder geometry (Couette geometry) with a temperature fixed at 298 K and a shear rate varying between $10^{-3}\,s^{-1}$ and $50\,s^{-1}$. The viscosity value $\eta_0$ was determined from the Newtonian plateau at low shear rates.

Several fibrin–chitosan formulations were then prepared by mixing solutions of 80 mg/mL fibrinogen, 3 M sodium chloride, 0.4 M calcium chloride, 1% chitosan, and 4 U/mL thrombin, in appropriate proportions to obtain fibrin and chitosan final concentrations of 10 mg/mL and 0.1–0.5%, respectively, into the hydrogel. The viscoelastic behavior of these formulations was investigated in a dynamic mode by using a 25 mm parallel plate geometry. The linear domain was determined by a strain sweep test at an angular frequency of 10 rad/s. The strain amplitude was then fixed at 1 %. Measurements of storage and loss moduli were then performed over time to evaluate the crossing point between these two moduli, indicative of the gel point.

For fibrin-alone and fibrin–chitosan hydrogel characterization with scanning electron microscopy, samples were prepared by mixing solutions of 80 mg/mL fibrinogen, 3 M sodium chloride, 0.4 M calcium chloride, phosphate-buffered saline (PBS; for fibrin-alone hydrogels) or 1% chitosan (for fibrin–chitosan hydrogels), and finally 4 U/mL thrombin, in appropriate proportions to obtain fibrin and chitosan final concentrations of 10 mg/mL and 0.5%, respectively, into the hydrogel. 35 μL of the mix were then injected into small cylindrical-conical plastic molds (7 mm long and 1–1.5 mm wide). After gelation, molds containing hydrogels were placed in 24-well dishes and covered with the SPE-IV/EBM® medium used for experiments with DP-MSC-populated hydrogels. Hydrogels were maintained in this medium for 7 days, and then fixed in 2% glutaraldehyde in 0.1 M sodium cacodylate buffer at room temperature (RT) for 4 h. After washing, samples were post-fixed in 1% osmium tetroxide for 1 h, dehydrated by critical point drying (CPD300; Leica, Solms, Germany), mounted on aluminum stubs, sputter-coated with a layer of copper using a MED020 sputter coater (Oerlikon Balzers, Kapfenberg, Austria), and observed under a Quanta 250 scanning electron microscope (FEI, Eindhoven, Netherlands) at 15 kV.

### 2.3. *Determination of the antibacterial effect of chitosan*

*Enterococcus fæcalis* (ATCC 29212) was cultured in Brain Heart Infusion broth (BHI, BioMérieux, Marcy-L'Etoile, France) at 37 °C overnight. The bacterial suspension was then diluted in BHI to obtain concentrations of approximately $2 \times 10^3$ Colony-Forming Units (CFU)/mL. The final bacterial solution was plated on agar plates after each experiment to ensure that the right bacterial concentration had been used. Fibrin-alone and fibrin–chitosan hydrogels were prepared as described above and cast in a 96-well plate (70 μL per well). After gelation, 150 μL of the bacterial suspension was added to the hydrogel-containing wells, as well as to empty wells for controls, and the plate was incubated at 37 °C for 6 h. Bacterial suspensions were then harvested, diluted and plated on Trypticase Soy Agar (TSA; Biomérieux) with a EasySpiral automated plater (Interscience, Saint-Nom-la-Bretèche, France). CFUs were counted with a Scan 1200 automated plate reader (Interscience) after plate incubation at 37 °C for 18 h.

### 2.4. *Dental Pulp-Mesenchymal Stem/stromal Cell (DP-MSC) isolation and expansion*

Isolation and expansion of DP-MSCs were performed as described by Ducret et al. [33]. Healthy impacted human third molars were collected from donors aged 13-17 years with informed consent of the patients and their parents, in accordance with the World Medical Association's Declaration of Helsinki and the French Public Health Code (Article R1211-49), and following a protocol approved by the French Ministry of Higher Education and Research (CODECOH: DC-2014-2325). Dental pulps from teeth between Nolla developmental stages 5 (crown almost completed) and 7 (one third root completed) were gently extirpated from pulp cavities and cut into fragments of about 0.5–2 $mm^3$. Pulp fragments were seeded as explants on dishes pre-coated with a mixture of human placental collagens I and III at a final concentration of 0.5 $\mu g/cm^2$ and cultured in SPE-IV/EBM® medium. DP-MSCs outgrowing from the explants were passaged 4 times before being encapsulated into the hydrogels. Our flow cytometry experiments revealed that the whole amplified cell population was positive to the MSC markers CD10, CD13, CD29, CD44, CD49a, CD73, CD90, CD105, CD166 and HLA-ABC. A significant percentage of these cells also expressed the mesenchymal stem cell antigen MSCA-1 (about 50% of the cells), the marker of perivascular

MSCs CD146 (15%), and the marker of neural and muscular MSCs CD56 (80%) [33–35].

### 2.5. Preparation of cellularized hydrogels

Fibrin-alone and fibrin–chitosan cellularized hydrogels were prepared by mixing DP-MSCs suspended in SPE-IV/EBM® medium with 80 mg/mL fibrinogen, 3 M sodium chloride, 0.4 M calcium chloride, PBS (for fibrin-alone hydrogels) or 1% chitosan (for fibrin–chitosan hydrogels) solutions and 4 U/mL thrombin, to get final concentrations of 10 mg/mL fibrin, 0.5% chitosan and 5000 cells/μL into the hydrogels. Cell-containing formulations were immediately injected into the same plastic molds as above. Upon gelation, molds were placed in 24-well dishes and hydrogels were cultured in SPE-IV/EBM® medium for 7 days.

### 2.6. Viability and morphological and ultrastructural characterization of DP-MSCs within hydrogels

DP-MSC viability and morphological aspect were analyzed in fibrin-alone and fibrin–chitosan hydrogels, either immediately upon gelation or after 7 days of culture, with the Live/Dead® kit (Sigma-Aldrich) according to the manufacturer's instructions. For each condition (fibrin-alone and fibrin–chitosan), three cellularized hydrogels were performed with DP-MSCs cultured from 3 different third molars, each tooth originating from one different patient. Cellularized hydrogels were gently extruded from the molds, rinsed twice with PBS, and incubated in a PBS solution containing 0.2 μM calcein-AM and 0.2 μM PI at 37 °C for 15 min. Hydrogels were then observed under a Nikon Eclipse TE300 fluorescence microscope, their most central region was photographed, and the percentage of living (green) cells was determined in a 200 square pixels' surface with the Image J software.

Cell ultrastructure and pericellular environment were analyzed with transmission electron microscopy. Fibrin-alone and fibrin–chitosan hydrogels cellularized with DP-MSCs were fixed after 7 days of culture in 2% glutaraldehyde diluted in 0.1 M sodium cacodylate buffer at RT for 4 h. After washing, samples were post-fixed in 1% osmium tetroxide for 1 h, dehydrated in a graded series of ethanol and embedded in Epon resin. After polymerization, ultrathin sections were cut with a diamond knife, picked up with copper grids (300-mesh), and post-stained with uranyl acetate and lead citrate on a Leica Ultrostainer. After air drying, grids were observed under a Philips CM 120 transmission electron microscope at an acceleration voltage of 80 kV.

### 2.7. Cell proliferation and collagenous matrix production analysis with reverse transcription quantitative real-time polymerase chain reaction and immunohistochemistry

Expression of the genes coding for MKI67, the proliferation-related Ki-67 antigen, and for the alpha 1 chains of collagens type I and type III, two major structural components of the dental pulp ECM [36], was analyzed with reverse transcription quantitative real-time polymerase chain reaction (RT-qPCR) in DP-MSCs cultured in fibrin-alone or fibrin–chitosan hydrogels for 2, 4 or 7 days in SPE-IV/EBM® medium. Total RNA extraction was performed with the GenElute Single Cell RNA Purification kit (Sigma-Aldrich). Quality control of the extracted RNA was performed with 1 μl samples by measuring UV absorbance (Thermo Scientific Nanodrop 2000, USA). The quantity of the extracted RNA was determined from the absorbance at 260 nm using a spectrophotometer (Nanodrop 2000). RNA purity was determined from the ratio of absorbance (A@260/A@280 nm and A@260/A@230 nm >1.8 and <2.2). Equal amounts of total RNA (100 ng) were reverse-transcribed into single-stranded complementary DNA (cDNA) using the Prime Script RT reagent kit (Takara, Ozyme, Montigny-le-Bretonneux, France), in a T100 thermal cycler (Bio-Rad, Hercules, CA, USA). Reverse transcription (RT) was performed using thermo-cycling conditions according to manufacturer's instructions: 37 °C for 15 min, 85 °C for 10 s, and 4 °C until further use or freezing. Quantitative real-time PCR (qPCR) amplifications were performed in a Rotor-Gene Q PCR cycler (Qiagen, Courtabœuf, France), in a 20 μL reaction mix containing 10 μL Fast Start Universal SYBR green master (Roche, Mannheim, Germany), 4 μL RT template diluted 1:3 in sterile water, 300 nmol/L of each primer, and 4 μL sterile water. Thermal cycling conditions consisted of an initial denaturation step at 95° C for 10 min and then 40–50 cycles of 95 °C for 10 s, and a final annealing/extension step at 60 °C for 20 s. The ribosomal protein L13a housekeeping gene (*RPL13A*) was used for sample normalization. Primers for *MKI67* and *COL3A1* genes were designed using the Primer-Blast software (http://www.ncbi.nlm.nih.gov/BLAST). Primers for *COL1A1* and *RPL13A* were taken from publications [37,38]. Gene-specific primer sequences are listed in Table 1. All runs were performed in duplicate. The comparative threshold cycle method (ΔΔCt) was employed for the relative quantification of gene expression. The expression level of each target cDNA marker was normalized to the *RPL13A* cDNA. Data were expressed as mRNA expression levels given by the $2^{-(\Delta\Delta Ct)}$ method [39].

Detection of the proteins MKI67 and collagens type I and type III was performed in hydrogels cultured for 7 days by immunohistochemistry. Hydrogels were gently removed from the molds, fixed in acidified formal alcohol (AFA; Microm Microtech, Brignais, France) at RT for 24 h, dehydrated in ethanol, acetone and xylene and classically embedded in paraffin. Five-micrometer serial sections were then cut, deparaffinized and rehydrated. For MKI67 immunodetection, antigen retrieval was carried out by microwaving sections (230 watts) in pH 6, 10 mM citrate buffer for 20 min. For collagen type I and collagen type III antigen retrieval, sections were incubated in 0.5% hyaluronidase diluted in PBS at RT for 1 h. After rinsing, sections were incubated with the anti-MKI67 rabbit recombinant monoclonal antibody (dilution 1/200 in PBS-3% bovine serum albumin [BSA]), the anti-type I collagen rabbit polyclonal antibody (1/2000) or the anti-type III collagen mouse monoclonal antibody (1/2000) at 4 °C overnight. After rinsing in PBS, endogenous peroxidase activity was blocked by incubation in 0.5% hydrogen peroxide at RT for 20 min. Antibody detection was then performed by incubating sections with horseradish peroxidase-conjugated secondary antibodies diluted in PBS-3% BSA (anti-rabbit Dako

**Table 1 – Gene-specific primer sequences used for RT-qPCR analysis.**

| Gene | Primer | Sequence | Amplicon size | Accession number |
|---|---|---|---|---|
| *MKI67* | Forward | 5′-CGTCCCAGTGGAAGAGTTGT-3′ | 70 bp | NM_002417 |
| | Reverse | 5′-CGACCCCGCTCCTTTTGATA-3′ | | |
| *COL1A1* | Forward | 5′-CAGCCGCTTCACCTACAGC-3′ | 83 bp | NM_000088.3 |
| | Reverse | 5′-TTTTGTATTCAATCACTGTCTTGCC-3′ | | |
| *COL3A1* | Forward | 5′-TCAAGGCTGAAGGAAATAGCAA-3′ | 70 bp | NM_000090.3 |
| | Reverse | 5′-TCCCCAGTGTGTTTCGTGC-3′ | | |
| *RPL13A* | Forward | 5′-AAAAAGCGGATGGTGGTTC-3′ | 168 bp | NM_012423.3 |
| | Reverse | 5′-CTTCCGGTAGTGGATCTTGG-3′ | | |

EnVision+ System- HRP, ref. K4002, or anti-mouse Dako EnVision+ System- HRP, ref. K4000) at RT for 45 min. After rinsing in PBS, the staining was revealed by incubating sections in the peroxidase substrate 3,3′-diaminobenzidine (DAB Substrate Chromogen System, ref. K3468; Dako-Agilent, Les Ulis, France) for 40–60 s. Sections were then slightly counterstained with Mayer's hematoxylin, mounted in aqueous medium and observed with a Leica DM2000 light microscope equipped with a DFC 450 camera. Images were acquired with the LASv4 software. Staining controls were performed by replacing primary antibodies either with PBS −3% BSA or with rabbit or mouse control IgGs. All these controls were negative (not shown).

### 2.8. *Statistical analysis*

Data are presented as the mean values ± standard deviation. Differences were analyzed using the Mann–Whitney U-test for nonparametric analysis. The number of independent samples from different donors (n) is indicated in figure captions. A *P* value <0.05 was considered to be significant.

## 3. Results

### 3.1. *Preparation and characterization of the chitosan solution, fibrin hydrogels and fibrin–chitosan hydrogels*

We first determined the concentrations of the chitosan solution that preserve a low viscosity of the final fibrin–chitosan formulation. This concentration was determined by measuring the viscosity of pH 7.2, 0.2–1% chitosan solutions. Our results showed that a chitosan concentration below 0.6% showed a relatively low viscosity (Fig. 1A). From this value, the viscosity strongly increased. We then performed rheological measurements to determine whether the gelation time of fibrin–chitosan formulations with 0.1–0.5% chitosan concentrations was clinically acceptable. We found that, before fibrinogen polymerization, the viscoelastic moduli G′(t) and G″(t) remained low and relatively stable, and then both moduli increased and G′(t) became significantly higher than G″(t) at longer times (Fig. 1B). The crossing point of the two curves pro-

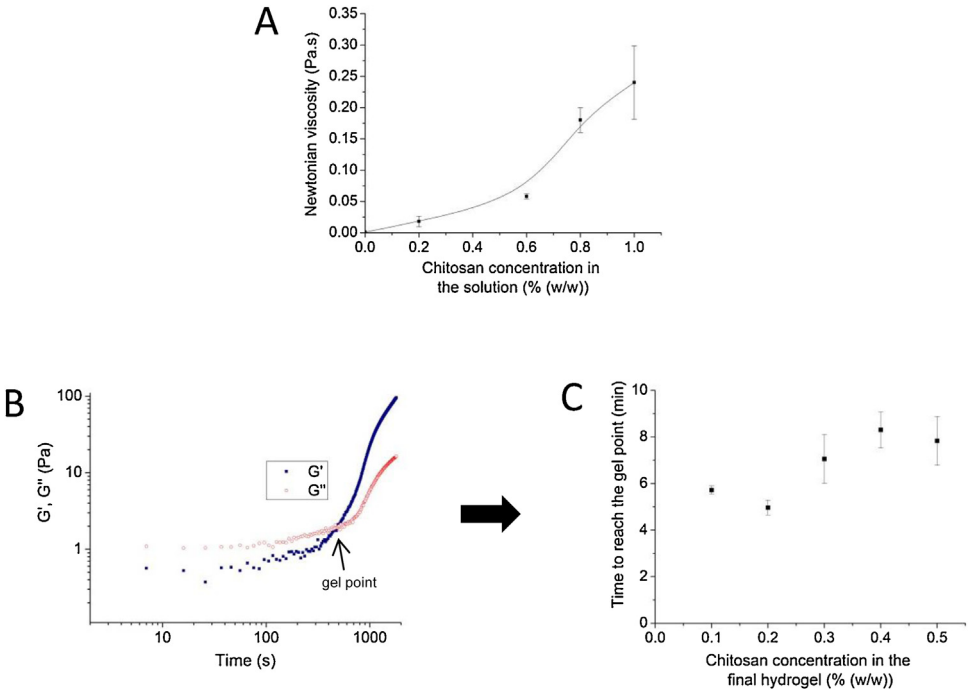


**Fig. 1 – Characterization of the chitosan solution and of fibrin–chitosan hydrogels. (A) Determination of the viscosity of pH 7.2, 0.2–1% chitosan solutions. Values are the mean ± standard deviation, n = 3. (B) An example of evolution of G′(t) and G″(t) viscoelastic moduli in a fibrinogen–chitosan formulation containing 0.5% [w/w] chitosan. (C) Time necessary to reach the gel point for 0.1–0.5% chitosan concentrations in the fibrin–chitosan formulation. Values are the mean ± standard deviation, n = 7.**

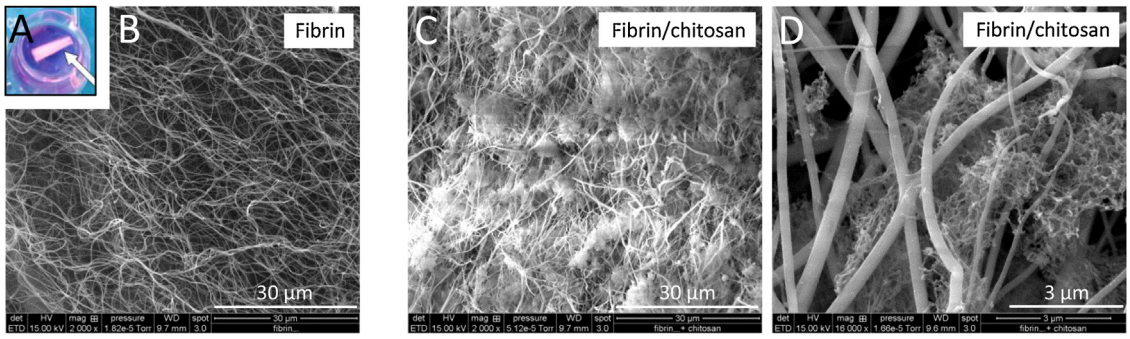


**Fig. 2 – Characterization of fibrin-alone and fibrin–chitosan hydrogels. (A) Photograph showing an example of hydrogel (opaque white) cast in a cylindrical-conical transparent plastic mold (white arrow) and covered with SPE-IV/EBM® medium. (B) Scanning electron microscopy showing the continuous fibrin network in a fibrin-alone hydrogel. (C) Rounded aggregates of chitosan trapped between and around the fibrin fibrils in the fibrin–chitosan hydrogel. (D) High magnification of a chitosan aggregate.**

vides an indication of the gelation time, in relation with the increasing number of physical junctions responsible for the formation of the fibrin gel network [40,41]. It was estimated here between 5 and 9 min, depending on the final concentration of chitosan entrapped into the fibrin network (Fig. 1C). Since all these times remained relevant to a clinical application, we decided to use for the remainder of the study the higher tested concentration of chitosan (0.5%) in the final formulation, in order to clearly exhibit the impact of the presence of chitosan in the final hydrogel.

Characterization of fibrin-alone hydrogels (Fig. 2A) with scanning electron microscopy after 7 days in SPE-IV/EBM® medium revealed a continuous network of fibrin fibrils (Fig. 2B). Chitosan addition resulted in the formation of rounded aggregates of chitosan entrapped in the fibrin network which was not altered (Fig. 2C and 2D).

### 3.2. *Determination of the antibacterial effect of chitosan incorporated into the fibrin hydrogel*

Bacterial growth was classically determined by counting CFUs after automated plating on agar plates (Fig. 3A and B). In the absence of hydrogel (control condition), *E. fæcalis* mean final concentration was found to be $4.60 \times 10^7$ CFU/mL after 6 h of incubation. When bacteria were grown with fibrin-alone hydrogels, the final bacterial concentration was $9.57 \times 10^7$ CFU/mL ($p = 0.0642$ versus control). When bacteria were grown with fibrin–chitosan hydrogels, their final concentration was significantly reduced ($3.74 \times 10^6$ CFU/mL) when compared to control or fibrin-alone conditions ($p < 0.0001$).

### 3.3. *Morphology, viability and proliferation of DP-MSCs cultured within hydrogels*

Encapsulated DP-MSCs were analyzed within either type of hydrogels, immediately after gelation or after 7 days of culture. At Day 0, living (green) DP-MSCs displayed a rounded morphology in fibrin–chitosan hydrogels (Fig. 4A), whereas, at Day 7, living cells were mostly elongated and fibroblast-like (Fig. 4B). Results were similar in fibrin-alone hydrogels (data not shown). The percentage of viable DP-MSCs (relative to the total number of DP-MSCs) was similar in fibrin-alone and fibrin–chitosan hydrogels, both at the beginning (Day 0) and at the end (Day 7) of culture (Fig. 4C). Cell proliferation was assessed by the expression of the nuclear marker MKI67 both at gene and protein level with RT-qPCR and immunohistochemistry, respectively. Compared to fibrin-alone hydrogels, *MKI67* gene expression was lower in fibrin–chitosan hydrogels after 2 days of culture but similar after 4 and 7 days of culture (Fig. 4D). The mean level of expression increased significantly between Day 2 and Day 4 of culture in fibrin–chitosan hydrogels. Proliferating cells were visualized after 7 days of culture by immunostaining of MKI67 with a specific antibody. Only rare DP-MSCs were labelled in both fibrin-alone and fibrin–chitosan hydrogels (Fig. 4E and F).

### 3.4. *Ultrastructural characterization of DP-MSCs within hydrogels*

The capacity of viable DP-MSCs to produce ECM components in fibrin-alone (Fig. 5 A–D) and fibrin–chitosan hydrogels (Fig. 5E–H) after 7 days of culture was then studied by transmission electron microscopy. The fibrin network was constituted by fibrils of different sizes (Fig. 5A). Chitosan formed rounded aggregates within the fibrin network (Fig. 5E). Special attention was paid to the cell cytoplasm in order to detect protein synthesis activity and to the close pericellular environment to determine whether cells were able to secrete collagenous components. Results indicated that DP-MSCs possessed, in both types of hydrogels, an abundant rough endoplasmic reticulum (Fig. 5B, C, F and G). Collagen fibers, recognizable by their characteristic 67 nm periodic cross-striation, were observed in the pericellular environment (Fig. 5D and H).

### 3.5. *Collagenous matrix production by DP-MSCs within hydrogels*

Since collagens type I and type III are major structural components of the dental pulp ECM, we studied their expression by DP-MSCs in fibrin-alone and fibrin–chitosan hydrogels at both gene and protein level. Expression of genes coding for collagen type I and collagen type III alpha 1 chains (*COL1A1* and

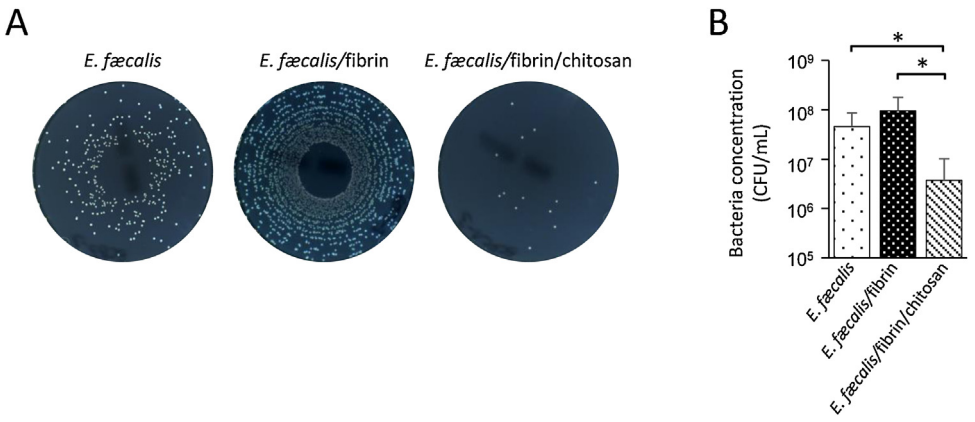


**Fig. 3 – Determination of the antibacterial effect of chitosan. The effect of chitosan was determined by comparing the growth of *E. fæcalis* bacteria in contact with fibrin-alone and fibrin–chitosan hydrogels. (A) Representative photographs of *E. fæcalis* CFUs incubated at 37 °C for 18 h on agar plates. The left picture shows CFUs obtained after the growth of bacteria in the absence of hydrogel (control). (B) Bacterial concentrations determined by CFU counting. Values are the mean ± standard deviation, n = 3. *p < 0.0001.**

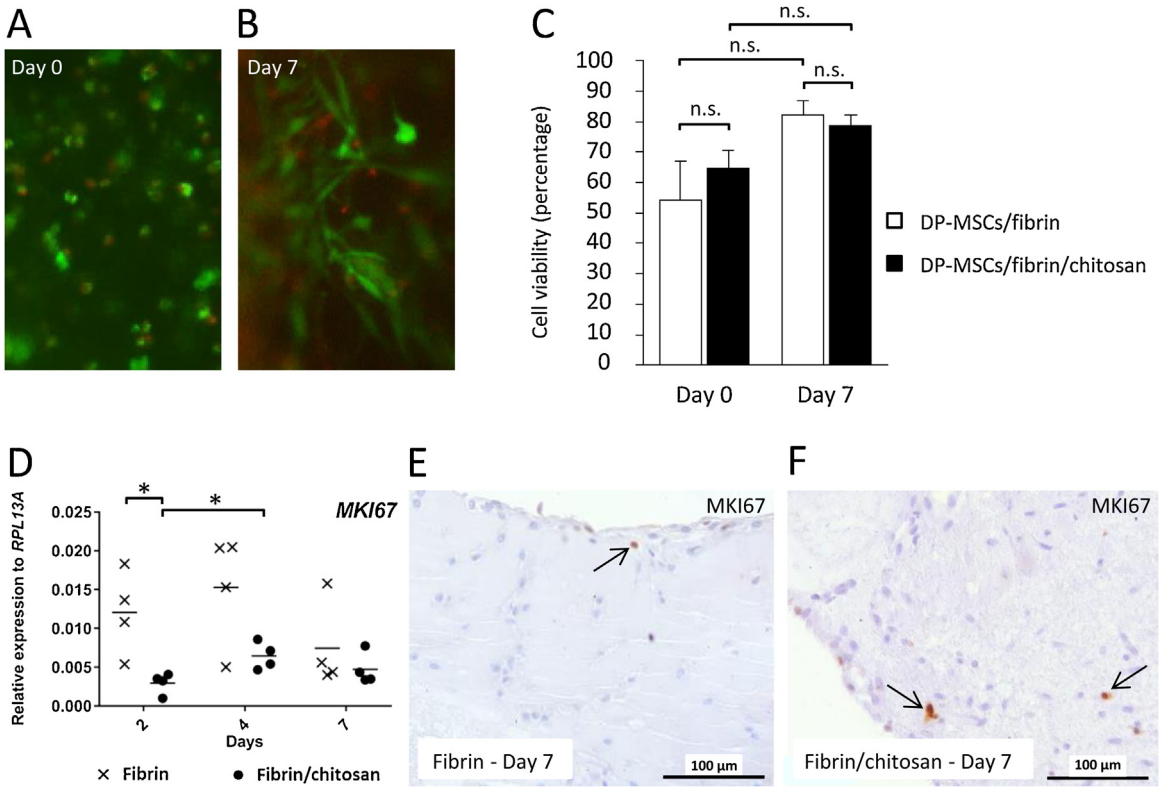


**Fig. 4 – Morphology, viability and proliferation of DP-MSCs cultured within hydrogels. Representative picture of DP-MSCs in a fibrin–chitosan hydrogel stained with the LiveDead kit® 2 h upon gelation (A; Day 0) and after 7 days of culture (B; Day 7). Dead cells were identified by the red nuclear staining resulting from the nuclear accumulation of propidium iodide. Viable cells were identified by the green cytoplasmic staining resulting from the cytoplasmic accumulation of calcein. (C) Percentage of viable DP-MSCs (relative to the total number of DP-MSCs). Values are the mean ± standard deviation, n = 3. n.s.: not significant. (D) Expression of the proliferation marker gene *MKI67* in fibrin-alone and fibrin–chitosan hydrogels after 2, 4 and 7 days of culture. Values are the mean ± standard deviation, n = 4. *p < 0.05. (E and F) Proliferating cells visualized after 7 days of culture by MKI67 immunostaining. (For interpretation of the references to colour in this figure legend, the reader is referred to the web version of this article.)**

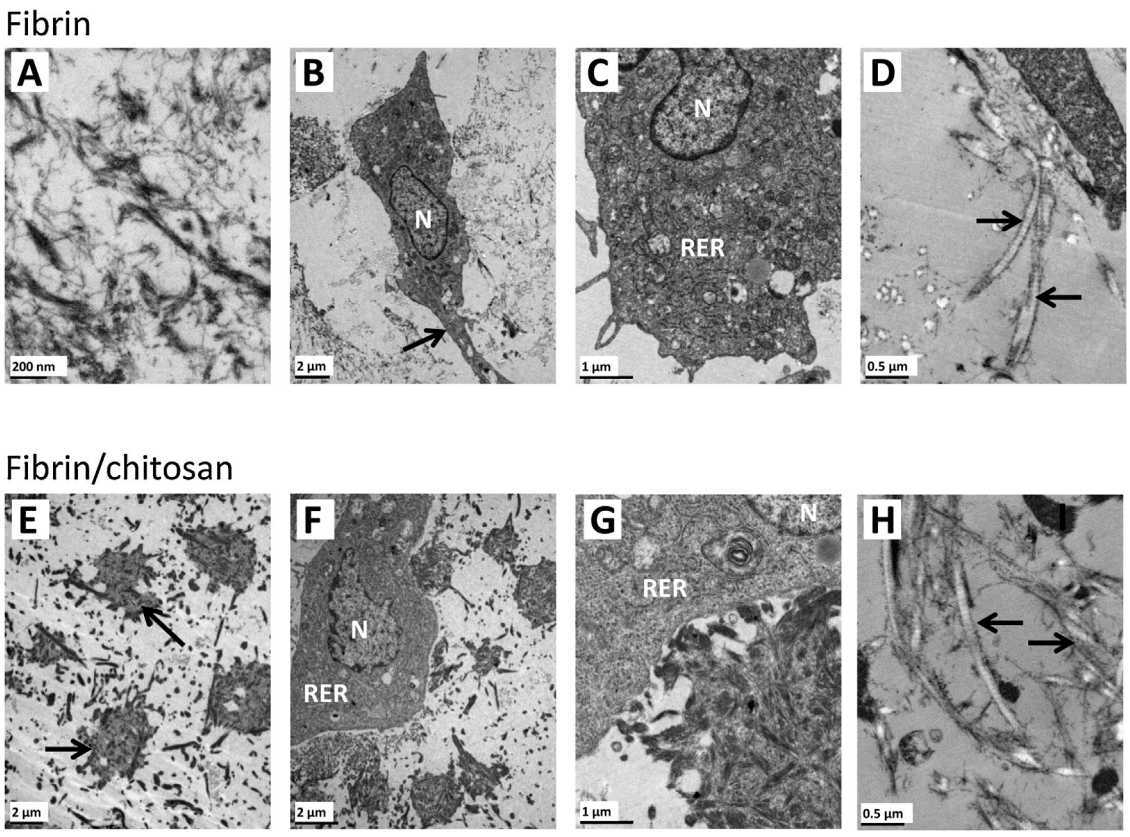


**Fig. 5 – Ultrastructural characterization of viable DP-MSCs and their pericellular environment within fibrin-alone and fibrin–chitosan hydrogels at Day 7. (A) Fibrin fibrils. (B) Fibroblast-like DP-MSC with an elongated cellular process (arrow). N: nucleus. (C) DP-MSC cytoplasm showing a well-developed rough endoplasmic reticulum (RER). (D) Collagen fibers (arrows) in the pericellular environment. (E) Rounded chitosan aggregates (dark grey; two are indicated by black arrows) within the fibrin network. (F) Fibroblast-like DP-MSC with a well-developed rough endoplasmic reticulum. (G) Close contact between a DP-MSC and a chitosan aggregate. (H) Collagen fibers (arrows) in the pericellular environment.**

*COL3A1*) was analyzed with RT-qPCR after 2, 4 and 7 days of culture, and collagen type I and type III proteins were detected with immunohistochemistry after 7 days of culture. We found that *COL1A1* gene expression was significantly higher at Day 2 in fibrin-alone hydrogels compared to fibrin–chitosan hydrogels, but was similar at Day 4 and Day 7 (Fig. 6A). Collagen type I was immunolocalized close to DP-MSCs in both types of hydrogels (Fig. 6B and C). *COL3A1* gene expression was similar between both types of hydrogel at these same three time points (Fig. 6D). Collagen type III was also immunolocalized close to DP-MSCs after 7 days of culture (Fig. 6E and F).

## 4. Discussion

We report in this study the design and characterization of an innovative cellularized chitosan-supplemented fibrin hydrogel in a formulation which preserves chitosan antibacterial properties while promoting the formation of a DP-like connective tissue.

We first performed several tests to develop a chitosan solution of cytocompatible pH and sufficiently fluid to preserve the injectability of the final fibrin–chitosan formulation. Since the viscosity of a chitosan solution increases with polymer molar mass ($M_w$), we selected shrimp shell chitosan with a $M_w < 250$ kg/mol. To get a pH of the solution close to neutrality to avoid detrimental effects on cell viability, we were compelled to increase the pH of the solution after the acidic dissolution of chitosan in deionized water. We tested several batches of chitosans with 20%, 33% and 40% DA and we found that only the solution of chitosan with a 40%DA could be brought to pH neutrality without forming precipitates. This DA was accordingly selected for the rest of the study the results of which are reported here. We then assessed the viscosity of the chitosan–fibrin formulation and its gelation time. Indeed, a relatively low viscosity of the formulation is necessary to allow for easy injection into an emptied endodontic space with a millimeter range diameter, and an appropriate "setting time" is needed, not too fast to enable accurate injection of the formulation into the endodontic space and not too long to allow for the rapid implementation of the crown filling. Our results indicated that the viscosity of the DA40% chitosan solution remained moderated below a chitosan concentration of 0.6%. Above this value, viscosity sharply increased and no longer allowed for accurate hydrogel injection into the cylindrical-conical mold (not shown). Based on this finding, measurement of the time necessary to reach the gel point was performed for different fibrin–chitosan hydrogels with chitosan concentra-

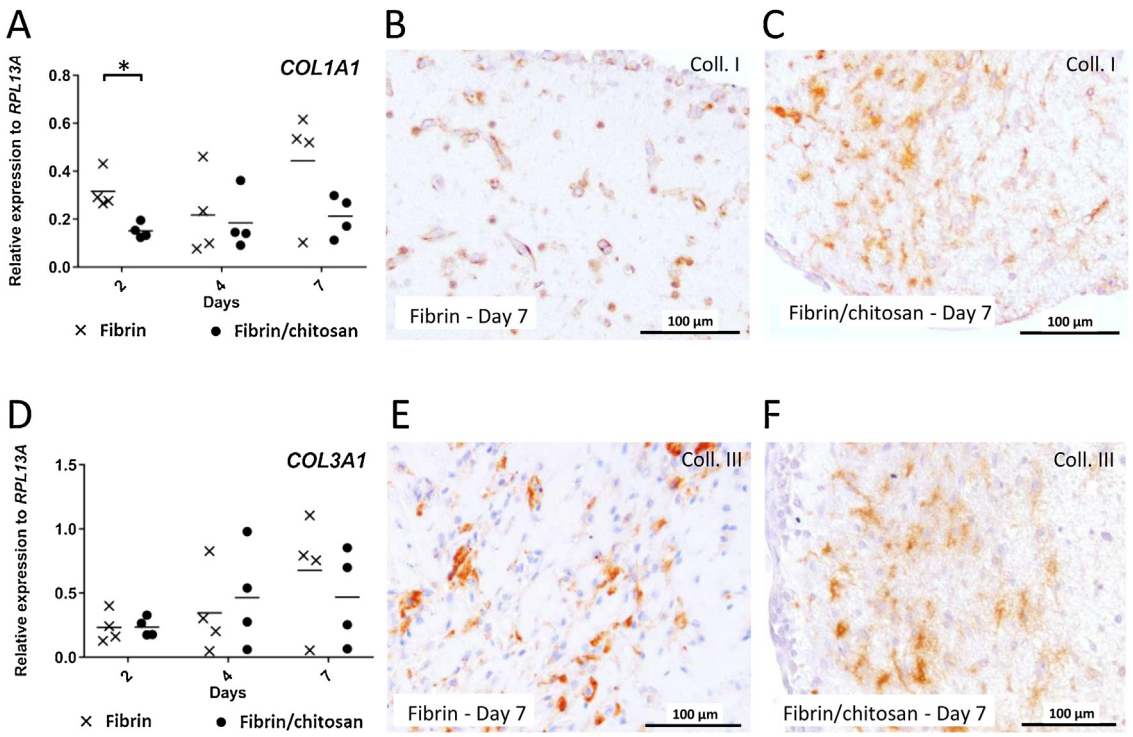


**Fig. 6 – Production of collagens type I and type III by DP-MSCs cultured in hydrogels. (A and D) Expression of *COL1A1* and *COL3A1* genes by DP-MSCs in fibrin-alone and fibrin–chitosan hydrogels after 2, 4 and 7 days of culture. Values are the mean ± standard deviation, n = 4. *p < 0.05. Immunolocalization of collagens type I (B and C) and type III (E and F) in both types of hydrogels after 7 days of culture.**

tions varying from 0.1 to 0.5% w/w. Our results indicated that this time was ranging between 5 and 9 min, which remained relevant to clinical application since it could allow slow injection of the formulation into the endodontic space of a one- to three-rooted human tooth. Accordingly, a final concentration of 0.5% chitosan was selected for the rest of the study.

The success of an endodontic treatment relies on the complete elimination of microorganisms present in the infected endodontic space. However, total disinfection can hardly be obtained with classical endodontic irrigants such as sodium hypochlorite, because of the complex anatomy of the root canal system and the limited penetrability of irrigants into the dentin tubules [42–44]. In this context, chitosan, given its known antibacterial properties, might be a good candidate to prevent the invasion of the fibrin scaffold by endodontic residual bacteria that could impair the DP regenerative process. In the field of dentistry, chitosan antibacterial effects have been assessed in the form of chitosan solutions, gels or nanoparticules mainly on *E. fæcalis*, a pathogen highly resistant to endodontic disinfectants and which is frequently found in persistent root canal infections [26,27,45,46]. Our findings showed that incorporation of DA40% chitosan into the fibrin network was able to limit the growth of *E. fæcalis* bacteria in contact with the hydrogel. Further experiments are needed (i) to test the antimicrobial activity of this scaffold against other bacteria present in the infected endodontic space, and (ii) to confirm that the chitosan can be released from the hydrogel to kill bacteria present either on the root canal dentin wall or in dentin tubules.

Tissue engineering studies have revealed that chitosan is highly biocompatible [47]. However, Kim et al. [48] have reported that chitosan alone did not significantly support human DP cell adhesion, proliferation or differentiation. The addition of chitosan/hyaluronic acid or chitosan/pectin scaffolds to apical bleeding during revascularization procedures in dogs did not improve the regeneration of a pulp-dentin complex [14]. However, fibronectin/chitosan scaffolds were shown to promote DP stem cell attachment and proliferation [49], suggesting that chitosan association to fibronectin was not deleterious to the cells. In the present work we observed that addition of chitosan to a fibrin-based scaffold did not alter DP-MSC survival, spreading, proliferation, and collagenous matrix production. In particular, the level of cell viability was high and similar to that observed for mesenchymal stem cells, including DP-MSCs, seeded in a fibrin scaffold [9,10,50]. Based on *MKI67* gene expression, DP-MSC proliferation was significantly higher in fibrin-alone hydrogels than in fibrin–chitosan hydrogels after 2 days of culture, suggesting that chitosan limited cell proliferation at the beginning of the culture. Such limitation rapidly faded with time, because *MKI67* gene expression was similar in fibrin-alone and fibrin–chitosan hydrogels after 4 days of culture. The number of proliferative DP-MSCs was very low at Day 7 in both fibrin-alone and fibrin–chitosan hydrogels, suggesting that cells had begun to differentiate.

The morphology of DP-MSCs incorporated in both hydrogels was mostly elongated and spindle-like after 7 days of culture, close to that of DP fibroblasts [51]. The early expression of collagen genes, soon after the beginning of cell culture

within hydrogels, suggested that DP-MSCs in the fibrin-alone and fibrin–chitosan scaffolds were rapidly in favorable conditions to create a three-dimensional collagenous environment resembling their native tissue. Electron microscopy analysis after one week of culture indicated that cells were highly active, as shown by the presence of a well-developed rough endoplasmic reticulum and deposition of collagen fibers in the cell vicinity.

Together these results suggest that the association fibrin–chitosan in the form of a hydrogel could promote cell-based DP regeneration by maintaining a bacteria-free environment in the endodontic space. They are in line with our recently published data reporting *ad integrum* regeneration of the colonic wall following implantation of fibrin–chitosan hydrogels cellularized with the stromal vascular fraction derived from the adipose tissue [52]. Cellularized fibrin–chitosan formulations could thus be used to regenerate various human tissues.

## 5. Conclusion

This study demonstrated that incorporating chitosan to a fibrin hydrogel confers the latter antibacterial properties which might prove helpful in endodontic space disinfection, without significantly altering the pro-regenerative properties of the fibrin scaffold. Further studies investigating this antibacterial effect should now be performed by using well-established monospecies or, better yet, multispecies biofilms similar to that present in the infected root canal. *In vivo* studies are also required to confirm these promising results and the interest of this scaffold for regenerative endodontics.

## Acknowledgements

This work was supported by the Gueules Cassées foundation, the French Institute for Odontological Research, the French National Centre for Scientific Research (CNRS) and the French Ministry of Higher Education and Research. The authors acknowledge the contribution of the *Centre Technologique des Microstructures* (Université Lyon 1, Villeurbanne, France) for help with electron microscopy and Novotec (Bron, France) for help with immunohistochemistry.

## REFERENCES

[1] Ng YL, Mann V, Gulabivala K. Tooth survival following non-surgical root canal treatment: a systematic review of the literature. Int Endod J 2010;43(3):171–89.
[2] Kim SG, Zhou J, Ling L, Cho S, Suzuki T, Fu SY, et al. Regenerative endodontics: barriers and strategies for clinical translation. Dent Clin North Am 2012;56(3):639–49.
[3] Hargreaves KM, Diogenes A, Teixeira FB. Treatment options: biological basis of regenerative endodontic procedures. J Endod 2013;39(3):30–43.
[4] Rosa V, Zhang Z, Grande RH, Nör JE. Dental pulp tissue engineering in full-length human root canals. J Dent Res 2013;92(11):970–5.
[5] Diogenes A, Ruparel NB, Shiloah Y, Hargreaves KM. Regenerative endodontics. A way forward. J Am Dent Assoc 2016;147(5):372–80.
[6] Gong T, Heng BC, Lo ECM, Zhang C. Current advance and future prospects of tissue engineering approach to dentin/pulp regenerative therapy. Stem Cells Int 2016;2016:9204574.
[7] Ducret M, Fabre H, Celle A, Mallein-Gerin F, Perrier-Groult E, Alliot-Licht B, et al. Current challenges in human tooth revitalization. Biomed Mater Eng 2017;28(S1):S159–68.
[8] Nakashima M, Iohara K, Murakami M, Nakamura H, Sato Y, Ariji Y, et al. Pulp regeneration by transplantation of dental pulp stem cells in pulpitis: a pilot clinical study. Stem Cell Res Ther 2017;8(1):61.
[9] Galler K, D'Souza RN, Hartgerink JD, Schmalz G. Scaffolds for dental pulp tissue engineering. Adv Dent Res 2011;23(3):333–9.
[10] Galler KM, Brandl FP, Kirchhof S, Widbiller M, Eidt A, Buchalla W, et al. Suitability of different natural and synthetic biomaterials for dental pulp tissue engineering. Tissue Eng A 2018;24(3–4):234–44.
[11] Demarco FF, Conde MC, Cavalcanti BN, Casagrande L, Sakai VT, Nör JE. Dental pulp tissue engineering. Braz Dent J 2011;22(1):3–13.
[12] Rosa V, Della Bona A, Cavalcanti BN, Nör JE. Tissue engineering: from research to dental clinics. Dent Mater 2012;28(4):341–8.
[13] Jones TD, Kefi A, Sun S, Cho M, Alapati SB. An optimized injectable hydrogel scaffold supports human dental pulp stem cell viability and spreading. Adv Med 2016;2016:7363579.
[14] Palma PJ, Ramos JC, Martins JB, Diogenes A, Figueiredo MH, Ferreira P, et al. Histologic evaluation of regenerative endodontic procedures with the use of chitosan scaffolds in immature dog teeth with apical periodontitis. J Endod 2017;43(8):1279–87.
[15] Albuquerque MTP, Valera MC, Nakashima M, Nör JE, Bottino MC. Tissue- engineering-based strategies for regenerative endodontics. J Dent Res 2014;93(12):1222–31.
[16] Janmey PA, Winer JP, Weisel JW. Fibrin gels and their clinical and bioengineering applications. J R Soc Interface 2009;6(30):1–10.
[17] Ruangsawasdi N, Zehnder M, Weber FE. Fibrin gel improves tissue ingrowth and cell differentiation in human immature premolars implanted in rats. J Endod 2014;40(2):246–50.
[18] Roura S, Gálvez-Montón C, Bayes-Genis A. Fibrin, the preferred scaffold for cell transplantation after myocardial infarction? An old molecule with a new life. J Tissue Eng Regen Med 2017;11(8):2304–13.
[19] Redl H, Schlag G, Stanek G, Hirschl A, Seelich T. In vitro properties of mixtures of fibrin seal and antibiotics. Biomaterials 1983;4(1):29–32.
[20] Fouad AF, Verma P. Healing after regenerative procedures with and without pulpal infection. J Endod 2014;40(4 Suppl):S58–64.
[21] Vishwanat L, Duong R, Takimoto K, Phillips L, Espitia CO, Diogenes A, et al. Effect of bacterial biofilm on the osteogenic differentiation of stem cells of apical papilla. J Endod 2017;43(6):916–22.
[22] Verma P, Nosrat A, Kim JR, Price JB, Wang P, Bair E, et al. Effect of residual bacteria on the outcome of pulp regeneration in vivo. J Dent Res 2017;96(1):100–6.
[23] Domard A. A perspective on 30 years research on chitin and chitosan. Carbohydr Polym 2011;84(2):696–703.
[24] Logith Kumar R, Keshav Narayan A, Dhivya S, Chawla A, Saravanan S, Selvamurugan N. A review of chitosan and its derivatives in bone tissue engineering. Carbohydr Polym 2016;20(151):172–88.

[25] Raafat D, Sahi H-G. Chitosan and its antimicrobial potential — a critical literature survey. Microb Biotechnol 2009;2(2):186–201.
[26] Shenoi PR, Morey ES, Makade CS, Gunwal MK, Khode RT, Wanmali SS. In vitro evaluation of the antimicrobial efficacy of chitosan and other endodontic irrigants against Enterococcus fæcalis. Gen Dent 2016;64(5):60–3.
[27] Shrestha A, Kishen A. Antibacterial nanoparticles in endodontics: a review. J Endod 2016;42(10):1417–26.
[28] Husain S, Al-Samadani KH, Najeeb S, Zafar MS, Khurshid Z, Zohaib S, et al. Chitosan biomaterials for current and potential dental applications. Materials (Basel) 2017;10(6):602.
[29] Hosseinnejad M, Jafari SM. Evaluation of different factors affecting antimicrobial properties of chitosan. Int J Biol Macromol 2016;85:467–75.
[30] Montembault A, Viton C, Domard A. Physico-chemical studies of the gelation of chitosan in a hydroalcoholic medium. Biomaterials 2005;26(8):933–43.
[31] Dumont M, Villet R, Guirand M, Montembault A, Delair T, Lack S, et al. Processing and antibacterial properties of chitosan-coated alginate fibers. Carbohydr Polym 2018;190:31–42.
[32] Vachoud L, Zydowick N, Domard A. Formation and characterization of a physical chitin gel. Carbohydr Res 1997;302:169–77.
[33] Ducret M, Fabre H, Farges J-C, Degoul O, Atzeni G, McGuckin C, et al. Production of human dental pulp cells with a medicinal manufacturing approach. J Endod 2015;41(9):1492–9.
[34] Ducret M, Fabre H, Degoul O, Atzeni G, McGuckin C, Forraz N, et al. Immunophenotyping reveals the diversity of human dental pulp mesenchymal stromal cells in vivo and their evolution upon in vitro amplification. Front Physiol 2016;7:512.
[35] Ducret M, Fabre H, Degoul O, Atzeni G, McGuckin C, Forraz N, et al. A standardized procedure to obtain mesenchymal stem/stromal cells from minimally manipulated dental pulp and Wharton's jelly samples. Bull Group Int Rech Sci Stomatol Odontol 2016;53(1):e37.
[36] Goldberg M, Smith AJ. Cells and extracellular matrices of dentin and pulp: a biological basis for repair and tissue engineering. Crit Rev Oral Biol Med 2004;15(1):13–27.
[37] Martin I, Jakob M, Schäfer D, Dick W, Spagnoli G, Heberer M. Quantitative analysis of gene expression in human articular cartilage from normal and osteoarthritic joints. Osteoarthritis Cartilage 2001;9(2):112–8.
[38] Pombo-Suarez M, Calaza M, Gomez-Reino JJ, Gonzalez A. Reference genes for normalization of gene expression studies in human osteoarthritic articular cartilage. BMC Mol Biol 2008;9:17.
[39] Livak KJ, Schmittgen TD. Analysis of relative gene expression data using real-time quantitative PCR and the $2^{-\Delta\Delta C}$T method. Methods 2001;25(4):402–8.
[40] Stauffer D, Coniglio A, Adam M. Gelation and critical phenomena. Adv Polymer Sci 1982;44(Polym Networks):103–58.
[41] Montembault A, Viton C, Domard A. Rheometric study of the gelation of chitosan in aqueous solution without cross-linking agent. Biomacromolecules 2005;6(2):653–62.
[42] Shrestha A, Shi Z, Neoh KG, Kishen A. Nanoparticulates for antibiofilm treatment and effect of aging on its antibacterial activity. J Endod 2010;36(6):1030–5.
[43] Rosen E, Tsesis I, Elbahary S, Storzi N, Kolodkin-Gal I. Eradication of *Enterococcus fæcalis* biofilms on human dentin. Front Microbiol 2016;7:2055.
[44] Neelakantan P, Romero M, Vera J, Daood U, Khan AU, Yan A, et al. Biofilms in endodontics — current status and future directions. Int J Mol Sci 2017;18(8), pii: E1748.
[45] Kishen A, Shi Z, Shrestha A, Neoh KG. An investigation on the antibacterial and antibiofilm efficacy of cationic nanoparticulates for root canal disinfection. J Endod 2008;34(12):1515–20.
[46] Ballal N, Kundabala M, Bhat K, Acharya S, Ballal M, Kumar R, et al. Susceptibility of *Candida albicans* and *Enterococcus fæcalis* to chitosan, Chlorhexidine gluconate and their combination in vitro. Aust Endod J 2009;35(1):29–33.
[47] Chedly J, Soares S, Montembault A, von Boxberg Y, Veron-Ravaille M, Mouffle C, et al. Physical chitosan microhydrogels as scaffolds for spinal cord injury restoration and axon regeneration. Biomaterials 2017;138:91–107.
[48] Kim NR, Lee DH, Chung PH, Yang HC. Distinct differentiation properties of human dental pulp cells on collagen, gelatin, and chitosan scaffolds. Oral Surg Oral Med Oral Pathol Oral Radiol Endod 2009;108(5):e94–100.
[49] Asghari Sana F, Çapkın Yurtsever M, Kaynak Bayrak G, Tunçay EÖ, Kiremitçi AS, Gümüşderelioğlu M. Spreading, proliferation and differentiation of human dental pulp stem cells on chitosan scaffolds immobilized with RGD or fibronectin. Cytotechnology 2017;69(4):617–30.
[50] Ho W, Tawil B, Dunn JC, Wu BM. The behavior of human mesenchymal stem cells in 3D fibrin clots: dependence on fibrinogen concentration and clot structure. Tissue Eng 2006;12(6):1587–95.
[51] Nancy A. Dentin-pulp complex. In: Nancy A, editor. Ten Cate's Oral Histology: development, structure and function. 8th ed. Saint-Louis, MO: Elsevier Mosby; 2013. p. 165–204.
[52] Denost Q, Pontallier A, Buscail E, Montembault A, Bareille R, Siadous R, et al. Colorectal wall regeneration resulting from the association of chitosan hydrogel and stromal vascular fraction from adipose tissue. J Biomed Mater Res A 2018;106(2):460–7.